

Figure 2: Block diagram of the feedback control system.

maximum voltage of ± 1000 volts are separated from the inputs via optocouplers [2].

2 CONTROL AND TRACKING

2.1 Flatness-based Controller

To calculate the voltages that have to be applied to the electrodes for following-up the desired trajectory, a droplet model including all significant forces is needed. Assuming the charged microdroplet to be a point charge Q and a spherical particle in the Stokes' flow regime the equation of motion is

$$m\ddot{\underline{q}} = (m - m_a)\underline{g} - 6\pi\eta r\dot{\underline{q}} + Q\underline{E}(\underline{q}, V_i). \quad (1)$$

Gravitational force, lifting force, friction force, and electrostatic force are regarded. The electric field $\underline{E}(\underline{q}, V_i)$ is a nonlinear function in the spatial coordinates $\underline{q} = (y, z)^T$ and the electric voltages V_i , $i = 1, \dots, 4$. Using the state vector $\underline{x} = (y, \dot{y}, z, \dot{z})^T$, the equation of motion can be rewritten as a nonlinear first-order differential equation system

$$\dot{\underline{x}} = \underline{A}\underline{x} + \underline{b}(\underline{x}, V_i) \quad (2)$$

with the matrix \underline{A} and vector \underline{b} calculated from Eqn. (1). To generate the electric field components E_y and E_z only two independent voltages $U_1 = V_1 = -V_3$ and $U_2 = V_2 = -V_4$ are required. Opposite electrodes are applied to opposite electric voltages to use the bipolar range of the high-voltage amplifier in an optimal way. Near the center of the electrode arrangement the electric field can be estimated in a good approximation by using a separation approach, linear in the two independent voltages $\underline{U} = (U_1, U_2)^T$, namely,

$$\underline{E}(\underline{q}, \underline{U}) = \underline{N}(\underline{q})\underline{U}. \quad (3)$$

The position depending components of the matrix \underline{N} are calculated by using finite-element method (ANSYS). Using the inverse \underline{N}^{-1} and Eqn. (1), the inputs \underline{U} of the control process can be expressed in terms of \underline{q} and the derivatives with respect to time $\dot{\underline{q}}$ and $\ddot{\underline{q}}$. This system satisfies the conditions of flatness [3], and therefore a flat output $\underline{y}_f = \underline{q} = (y, z)^T$ can be found with

$$\underline{x} = \underline{x}(\underline{y}_f, \dot{\underline{y}}_f), \quad \underline{U} = \underline{U}(\underline{y}_f, \dot{\underline{y}}_f, \ddot{\underline{y}}_f). \quad (4)$$

In this inverse dynamics problem, appropriate inputs \underline{U} can be determined to steer the control system by applying the desired trajectory $\underline{y}_{f,d}(t) = \underline{q}_d(t)$ and its derivatives with respect to time $\dot{\underline{y}}_{f,d}$ and $\ddot{\underline{y}}_{f,d}$ in Eqn. (4). To stabilize the system against different initial conditions in droplet position and velocity as well as perturbations, a state feedback controller for trajectory following-up was designed. Therefore new inputs \underline{v} are defined

$$\underline{v} = \ddot{\underline{y}}_f = \ddot{\underline{y}}_{f,d} - c_1(\underline{y}_f - \underline{y}_{f,d}) - c_2(\dot{\underline{y}}_f - \dot{\underline{y}}_{f,d}). \quad (5)$$

The constants c_1 and c_2 are determined to achieve an asymptotic stable following-up error $\underline{e}(t)$

$$\lim_{t \rightarrow \infty} \underline{e}(t) = \lim_{t \rightarrow \infty} (\underline{y}_f(t) - \underline{y}_{f,d}(t)) = \underline{0} \quad (6)$$

If the position $(y, z)^T$ and velocity components $(\dot{y}, \dot{z})^T$ of the microdroplet are known at every point of time, the voltages \underline{U} to allow trajectory following-up of $\underline{y}_{f,d}(t)$ can simply be determined using Eqn. (5) and Eqn. (4) (left part of Fig. 2). The camera system, however, only supplies the position of the droplet at discrete points of time and no information about the velocity components. Therefore a so-called observer has to be applied

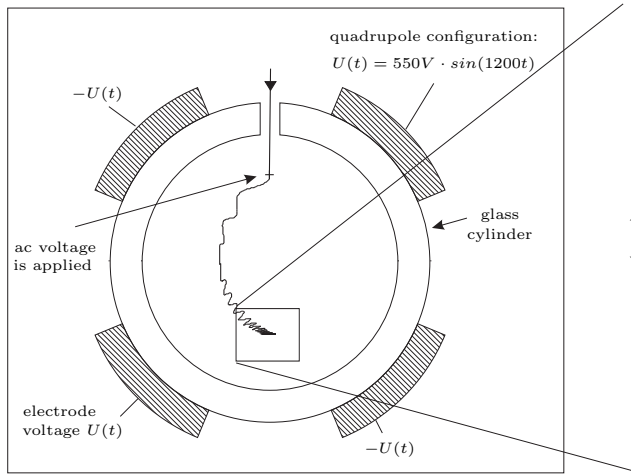


Figure 3: Trajectory of a charged microdroplet in an electric field of quadrupole character.

to estimate the components of the state vector which cannot be directly measured (actual position and velocity, right part of Fig. 2). This estimated state vector \hat{x} can now be used to determine the voltages for trajectory following-up.

2.2 Microdroplet Tracking

Due to the image generation and read-out process, the actual droplet position is different from the captured image. To predict the actual position and velocity of the droplet, the observer has to integrate the second order differential equation of motion using a fast approximation algorithm. Therefore initial conditions of position and velocity are required and also the time dependence of the electric field. Defined initial conditions for the tracking can be obtained by applying a two-phase ac voltage according to conventional electrodynamic levitation traps [4] after the microdroplet is dispensed. The expulsion velocity of about 1.5 m/s at the nozzle is too high to trap the microdroplet using the camera system with a data rate of about 100 position and timestamp information per second (if the whole image is processed). Fig. 3 shows a simulated trajectory of a charged microdroplet in the time depending quadrupole potential. The single droplet with a diameter of 65 μm , an initial velocity of 1.5 m/s at the dispenser and $1 \cdot 10^6$ charge carrier is slowed down and trapped near the center of the camera image. The microdroplet oscillates with a small amplitude and a phase shift of π according to the driving electrode voltage $U(t)$. Regarding this phase shift, together with the fact of a maximum in probability density at the reversal points of a harmonic oscillation, the camera system is able to capture the droplet at such a reversal point. By processing this starting image with

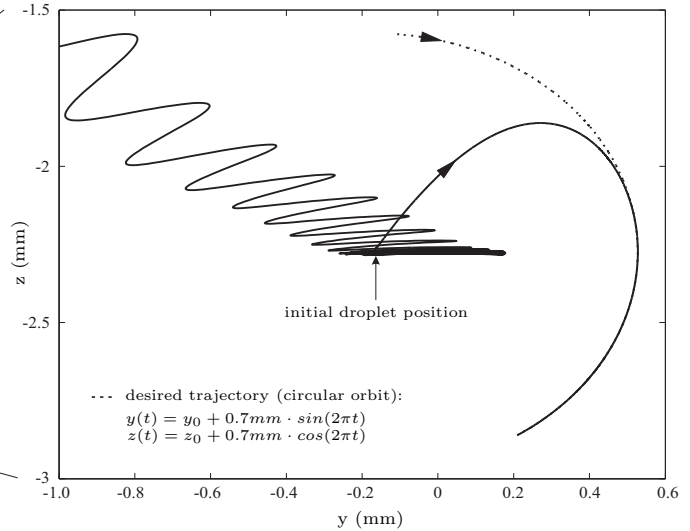


Figure 4: Closeup of the trajectory simulation.

the timestamp t_1 , all initial conditions of position but also velocity can be determined exactly. After the position information has been transferred, all voltages are switched off and the tracking algorithm is started at the point of time t_2 when the microdroplet reaches the reversal point next. Regarding the desired trajectory, the follow-up controller is now able to calculate the voltages \underline{U} . After these voltage values have been sent to the Digital-to-Analog Converter, the tracking algorithm estimates the actual state vector using the explicit Euler method and the approximated electric field according to Eqn. (3). The trajectory prediction and voltage calculation steps are carried on until new position and timestamp information arrives at the observer. Generally, when the camera starts exposing a new image at t_k , at the same time the tracking algorithm stores the actual predicted position and velocity to compare the data when the according image information is transferred from the camera some milliseconds later at t_{k+1} . Until this position information arrives at the observer, the follow-up controller uses the estimated state vector \hat{x} of the tracking for the feedback-control. When the position information from the camera according to time t_k arrives at the observer at t_{k+1} , the actual predicted position at time t_{k+1} can be estimated again. First of all, the predicted velocity $\hat{v}(t_k)$ of the tracking is adapted ($\hat{v}_{ad}(t_k)$). Therefore the primary value $\hat{v}(t_k)$ and the velocity $\underline{v}_c(t_k)$, determined from the last three measured positions at t_k, t_{k-1} and t_{k-2} , $k \geq 3$, with their according timestamps are used

$$\hat{v}_{ad}(t_k) = p\hat{v}(t_k) + (1-p)\underline{v}_c(t_k), \quad p = p(\hat{v}) \in [0, 1]. \quad (7)$$

If the estimated velocity of the charged microdroplet is high, $\hat{v}_{ad}(t_k)$ is mainly determined by the primary pre-

dicted one ($p(\hat{v}) \rightarrow 1$), because the calculation of the velocity components from measured positions and their timestamps can be very inaccurate due to the possibly high acceleration in the system compared to the difference in time between two images. Now, the actual position is estimated again ($(\hat{y}_{ad}(t_{k+1}), \hat{z}_{ad}(t_{k+1}))^T$). Therefore the predicted trajectory between t_k and t_{k+1} is added to the measured position $(y_c(t_k), z_c(t_k))^T$. In addition, the contribution of the reestimated velocity $\hat{v}_{ad}(t_k)$ is included by the term

$$(t_{k+1} - t_k) \cdot (\hat{v}_{ad}(t_k) - \hat{v}(t_k)). \quad (8)$$

Also, the actual prediction for the velocity $\hat{v}(t_{k+1})$ is adapted

$$\hat{v}_{ad}(t_{k+1}) = \hat{v}_{ad}(t_k) + (\hat{v}(t_{k+1}) - \hat{v}(t_k)). \quad (9)$$

This observer algorithm is very fast because no additional integration steps are required. The effects from an inhomogeneous electric field and an explicit velocity dependent friction force are neglected in the reestimation steps. Fig. 4 shows a simulated trajectory using the feedback control system with the desired trajectory as the dotted line and the calculated droplet trajectory using Runge-Kutta method with a fixed time step of 10 ns as the solid line. In this case of a given circular orbit with an angular frequency of $\omega = 2\pi$ 1/s at a diameter of 1.4 mm, trajectory following is obtained. Other simulations show that this trajectory following can also be reached at angular frequencies of the desired circular orbit up to $\omega = 2\pi \cdot 50$ 1/s.

3 EXPERIMENTAL RESULTS

As conducting liquid a solution of calcium chloride, ethylene glycol, and water is dispensed. The microdroplet is generated using a piezo actuator and during the expulsion process the electrostatic field of the electrode near the nozzle causes the droplet to be charged by induction. In order to determine the amount of induced excess charge carrier on the microdroplet two different methods have been applied. In the direct method, the droplets have been collected by a faraday cup which was connected to a calibrated, high-sensitive charge amplifier. In the second method, several positions of the droplet together with their timestamps have been recorded and the droplet charge was determined by comparison with the simulation of its trajectory in the electrostatic field using the droplet charge Q as a fitting parameter. Because of the complex modelling of the electrostatic field in the presence of a charged microdroplet near the nozzle, both in the range of a few micron, the error bars resulting from this method in Fig. 5 are large compared to the measurement using the charge amplifier. The mean values however are very well coincident and therefore the simulated trajectories of the flatness based feedback control system are significant. The

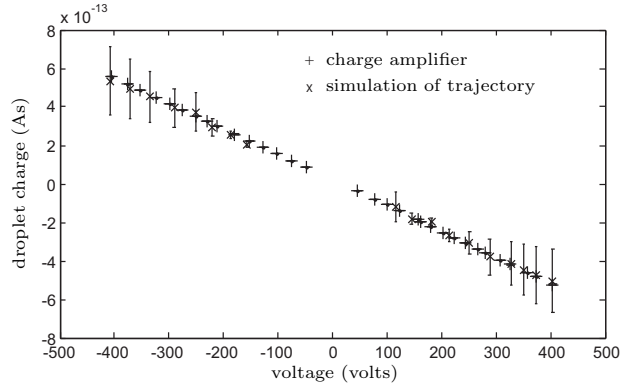


Figure 5: Droplet charge vs. induction voltage between electrode and dispenser nozzle.

droplet charge as the main simulation parameter can be determined sufficiently exact. The measured correlation between excess charge carrier on the microdroplet and induction voltage is in good agreement with experimental results using sodium chloride - water solutions [5].

The electrode arrangement and the applied voltages are determined to focus the charged microdroplet in the two dimensional object plane of the camera system. The setup can be extended in the third dimension perpendicular to that plane only by changing the algorithm of calculating the voltages in the following-up controller and the possibility of adjusting the object plane of the camera system. Therefore the trajectory of a charged microdroplet can be freely chosen in a two- or three-dimensional region, only acceleration and the according velocity is limited.

REFERENCES

- [1] D. J. Maloney et al., "Measurement and dynamic simulation of particle trajectories in an electrodynamic balance: Characterization of particle drag force coefficient/mass ratios," *Rev. Sci. Instrum.*, 66, 3615-3622, 1995.
- [2] V. Ström et al., "Inexpensive high-voltage low-current amplifier for driving long-range scanning tunneling microscope piezoactuators," *Meas. Sci. Technol.*, 6, 1072-1077, 1995.
- [3] Ph. Martin, R. M. Murray, P. Rouchon, "Flat systems," *European Control Conference*, Brussels, 1997.
- [4] R. F. Wuerker, H. Shelton, R. V. Langmuir, "Electrodynamic Containment of Charged Particles," *Jour. of Appl. Phys.*, 30, 342-349, 1958.
- [5] G. Reischl, W. John, and W. Devor, "Uniform electrical charging of monodisperse aerosols," *J. Aerosol Sci.*, 8, 55-65, 1977.